Chemistry & Biology, Vol. 11, 1643–1649, December, 2004, ©2004 Elsevier Ltd. All rights reserved. DOI 10.1016/j.chembiol.2004.09.014

Structures of End Products Resulting from Lesion Processing by a DNA Glycoylase/lyase

Sang J. Chung[1] and Gregory L. Verdine[1,2,*]
[1]Department of Chemistry and Chemical Biology
[2]Department of Molecular and Cellular Biology
Harvard University
Cambridge, Massachusetts 02138

Summary

DNA glycosylase/lyases initiate the repair of damaged nucleobases in the genome by catalyzing excision of aberrant nucleobases and nicking of the lesion-containing DNA strand. Nearly all of these proteins have the unusual property of remaining tightly bound in vitro to the end products of the reaction cascade. We have taken advantage of this property to crystallize and structurally characterize the end product resulting from complete DNA processing by a catalytically active mutant form of human 8-oxoguanine DNA glycosylase (D268E hOgg1). The resulting structure is consistent with the currently accepted catalytic mechanism for the protein. Unexpectedly, however, soaking of a nucleobase analog into the crystals results in religation of the DNA backbone in situ.

Introduction

DNA glycosylase/lyases are key components of the base excision DNA repair pathway, which is responsible for the eradication of damaged nucleobases from the genome [1, 2]. These proteins process their substrates in two distinct ways, catalyzing cleavage of the glycosidic bond linking the lesion nucleobase to its 2′-deoxyribose moiety (glycosylase activity), and scission of the DNA backbone on the 3′-side of the damaged site through a conjugate elimination mechanism (β-lyase activity) [3, 4]. Both of these enzymatic activities are now known to be mechanistically coupled through a covalent catalysis scheme (Figure 1) involving an essential amine-containing nucleophile on the enzyme [5], either the α-amino group of an *N*-terminal threonine [6] or proline [7] or the ε-amino group of an internal lysine [8, 9]. In either case, the overall repair reaction is unique for the sheer number of different sequential transformations it entails, all being catalyzed within the single active site of the DNA glycosylase/lyase enzyme. It is of fundamental interest in mechanistic enzymology to understand how the active sites of DNA glycosylase/lyases are constructed to achieve such remarkable catalytic versatility.

High-resolution structural studies on glycosylase/lyases bound to single-base lesions in DNA [10–12] have revealed that although these proteins fall into two known structural superfamilies, all recognize and repair their substrates by extruding the damaged nucleoside from the DNA helix and inserting it into an extrahelical active site on the enzyme. The largest superfamily of such proteins possesses a hallmark HhH-GPD structural motif comprising a helix-hairpin-helix (HhH) element followed directly by a Gly/Pro-rich loop and an invariant aspartic acid residue (GPD) element. The HhH-GPD glycosylase that has been most extensively studied with respect to structure/function relationships [10, 13–15] is 8-oxoguanine DNA glycosylase (Ogg1), which excises a highly mutagenic form of oxidatively damaged guanine from DNA. These structures have shed considerable light on the basis for specific lesion recognition by Ogg1 and on the early steps of the β-lyase reaction cascade. Particularly noteworthy is the discovery that the free oxoguanine (oxoG) nucleobase produced in the base excision step remains bound in the enzyme active site and acts as an acid/base cofactor to facilitate strand scission [15]. Structures representing the later steps of the β-lyase cascade are not yet available.

As part of ongoing efforts to elucidate the entire pathway of lesion search [16], recognition [10], and repair [13–15] by human Ogg1 (hOgg1), we have sought to obtain a structure of the complex formed between the enzyme and the DNA end product of its repair. Such a structural determination is made possible in principle by the fact that hOgg1, like most DNA glycosylases, remains tightly bound to its end product [17]. Although it has proven possible to obtain crystals of the end-product complex with wild-type hOgg1 that diffract to 2.8 Å resolution (unpublished data), the experimental electron density maps in the active site region have not proven unambiguously interpretable, owing perhaps to the modest resolution and presence of multiple end-product forms. Recently, we found unexpectedly that a mutant version of hOgg1 having the absolutely conserved aspartic acid residue, Asp268, mutated to glutamic acid (D268E hOgg1) retains full catalytic activity [14] and preserves the active site structure, except for the difference in side chain (Asp versus Glu) at position 268. Here we report that crystals of the end-product complex formed with the D268E mutant of hOgg1 yield clearly interpretable electron density maps. The structure of the end-product lesion is completely dependent upon the occupancy of a nucleobase in the lesion recognition pocket. Remarkably, we observe that hOgg1 actually religates the cleaved DNA strand in the presence of a purine base analog. Below, we detail these structures and discuss their implications for the mechanism of DNA repair by hOgg1.

Results and Discussion

Structure of the End Product

Crystals of D268E hOgg1 bound to end-product DNA yielded diffraction data that enabled structural refinement to 2.30 Å resolution. The overall structure is nearly identical to that of the previously determined lesion-recognition complex [10] (heavy atom rmsd = 0.57 Å), with the differences being limited to the active site region. Simulated annealing omit maps in the active site region clearly show the absence of electron density for the excised oxoG base, indicating that the base has

*Correspondence: verdine@chemistry.harvard.edu

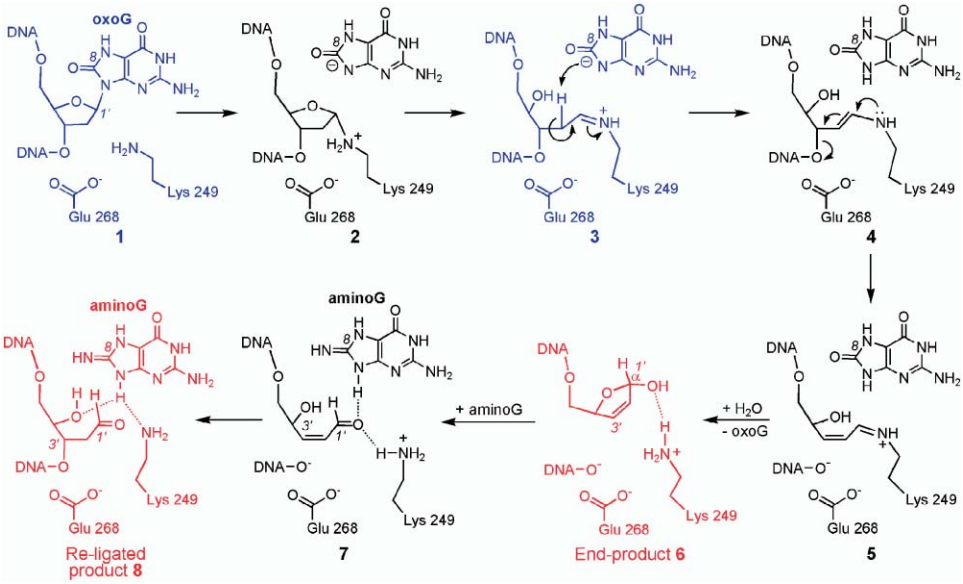

Figure 1. Proposed Mechanism for hOgg1-Catalyzed Excision of 8-Oxoguanine (oxoG) and Cleavage of the DNA Strand

Structures representing **1** [10] and **3** [15] have been determined in previous studies, and structures **6** and **8** have been determined in this work.

been released from its recognition pocket (Figure 2A). Although electron density is continuous from the sugar moiety of the end product to the side-chain of the catalytic nucleophile, Lys249, the two are separated by too great a distance to be connected by a covalent bond. This indicates that the enzyme has been released from the product by hydrolysis of the C1′=N$^{\epsilon}$ bond linking the two (refer to Figure 1), congruent with the accepted enzyme mechanism. Electron density is completely absent between C3′ of 2′,3′-didehydro-2′,3′-dideoxyribose (DDR) moiety and its 3′-phosphate (Figure 2A), and C3′ and its closest 3′-phosphate oxygen are separated by a distance (5.0 Å) far exceeding that of a phosphodiester P-O bond length (1.6 Å), consistent with the β-elimination reaction having proceeded to completion. Of the several candidate structures for the lesion sugar

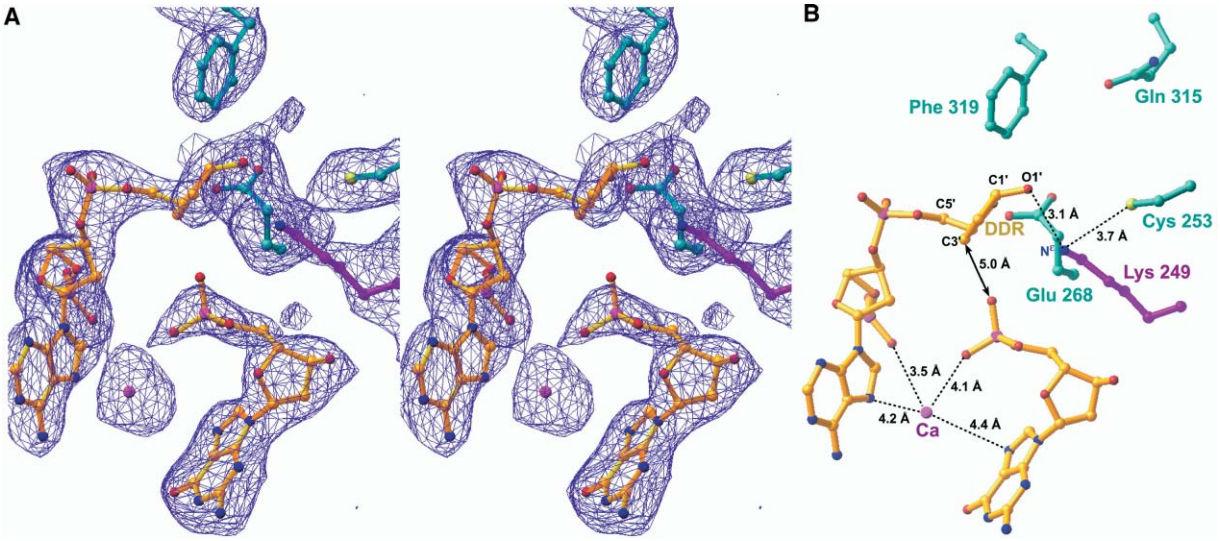

Figure 2. Active Site Structure of the End-Product Complex

(A) Fit of the end-product model to the $F_o - F_c$ electron density map refined to 2.30 Å and weighted using σA [27] coefficients. The map was calculated using simulated-annealing omit phases and contoured at 2.5 σ. Density corresponding to the oxoG base is absent. Note the interruption of density for the DNA backbone.

(B) Active site structure of the end-product crystal, with relevant distances indicated. Note the long distance between the 2′,3′-dehydro-2′,3′-dideoxyribose (DDR) moiety and the 3′-phosphate.

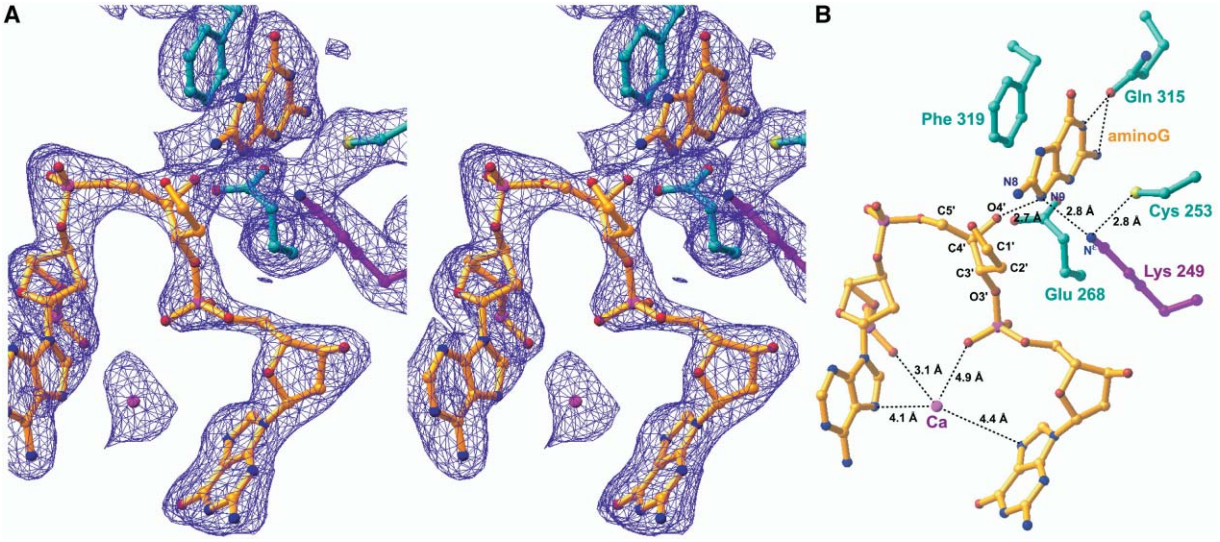

Figure 3. Active Site Structure of the Religated Complex

(A) Fit of the modeled religated product structure to its final $F_o - F_c$ electron density map (3 σ contour) refined to 1.90 Å and weighted as in Figure 2A. Density corresponding to aminoG is readily apparent in the base-recognition pocket. Note the continuous density in the DNA backbone. Electron density corresponding to the aldehyde (C1′ and O1′) or hydrated aldehyde in the ring-opened sugar is not present, suggesting that this portion of the structure is conformationally mobile. The extra density near N8 of aminoG could be due to an associated water molecule or buffer counterion, present at partial occupancy.

(B) Active site structure of the end-product crystal with 8-aminoguanine, with relevant distances indicated.

moiety of the end product, that which fits the electron density best is DDR (refer to Figure 1, structure **6**, and Figure 2A). The stereochemistry of the hydroxyl at C1′ in DDR appears to be α(*S*), as the model of the alternative β(*R*) isomer exhibited a poor fit with simulated annealing omit maps; this particular configuration appears to be stabilized by a hydrogen bond to the ϵ-amino group of Lys249 (N-O distance 3.1 Å; Figure 2B). The C2′=C3′ double bond in the DDR moiety clearly adopts the *cis* configuration; this does not necessarily indicate that the primary product of β-elimination (**5**) contains a *cis* olefin, as the double bond geometry might have undergone equilibration subsequent to its formation and been channeled to a more stable cyclized product. The Lys249 ϵ-amino also lies in reasonably close proximity to Cys253 (N-S distance 3.7 Å; Figure 2B), such that the two may be engaged in a weak hydrogen bond. A similar interaction between Cys253 and Lys249 has been observed in other structures of hOgg1, and has led us to suggest that this pair of residues might interact electrostatically with the departing oxoG nucleobase anion during glycosidic bond cleavage by an S_N1-type mechanism [14].

Cocrystal Structure in the Presence of a Nucleobase

The structure described above is that of an abasic complex. To investigate the influence of a nucleobase on the structure of the complex, we next soaked 8-aminoguanine (aminoG) into the cocrystals of the end-product complex, and refined the structure to 1.90 Å. Outside of the active site region, the structure of the amino G-containing complex is almost indistinguishable from that of the abasic end product (heavy atom rmsd = 0.44 Å). Electron density corresponding to aminoG is readily discernible in the active site of the soaked crystals (Figure 3A). The specific contacts between aminoG and residues of the base-recognition pocket are essentially identical to those seen previously for this analog in the structure of a covalently trapped catalytic intermediate [15], and also correspond directly to the contacts to oxoG observed in several cocomplexes representing different states of the overall repair reaction [10, 15]. A second major difference in the active site was completely unexpected. Whereas the abasic cocomplex contains a nick 3′ to the lesion, the complex soaked with aminoG exhibits strong, continuous density along the entire DNA backbone, consistent with its having a fully intact covalent structure. Thus, soaking of aminoG into the abasic crystals results not only in loading of the nucleobase into the active site, but also in religation of the nicked strand. The structure of the religated product was deduced by attempting to model all of the chemically accessible candidate structures into the electron density maps. This exercise was facilitated by the relatively high resolution of the structure, and by the clear density for the phosphates bracketing the lesion and for C5′, C4′, and O4′. Given these constraints, the modeled structure that provides the best fit to the diffraction data has the phosphate reattached at C3′. The stereogenic center at C3′ created by the reattachment process appears to have predominantly the α (*S*) configuration, as the alternative β (*R*) epimer yielded a substantially worse fit to the electron density maps. Density attributable to C2′ is visible in the maps, but that for the C1′=O aldehyde carbonyl (probably present as a hydrate) is not evident, even at the low contour level of 1.8 σ (not shown); absence of the car-

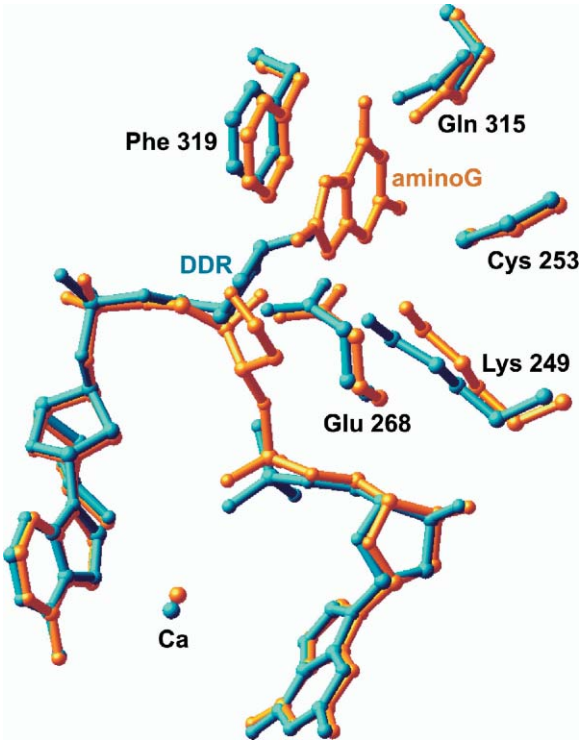

Figure 4. Superposition of the End Product and Religated Structures

Cyan, end product structures; gold, religated structures.

bonyl group is mechanistically impossible, so its absence from the electron density maps most likely results from a high degree of conformational mobility in this unconstrained segment of the open-chain sugar. As with all other hOgg1 structures containing a free nucleobase in the active site [15], our soaked structure shows a hydrogen bond between the sugar 4′-OH and the N9 of the purine nucleobase (O-N distance 2.7 Å; Figure 3B). Another feature of the present structure in common with previous structures is the hydrogen bonding interaction between the nucleobase N9 and the N^{ϵ} of Lys249 (N-N distance 2.8 Å; Figure 3B). As in the abasic end-product complex, the aminoG complex has a hydrogen bond between N^{ϵ} of Lys249 and the thiol of Cys253, but the distance in the latter case is considerably shorter (N-S distance 2.8 Å; Figure 3B).

Structural Implications for the Reaction Mechanism

Superposition of the abasic and aminoG-containing end-product structures reveals the similarities and differences between the two (Figure 4). Most of the active site residues on D268E hOgg1 adopt similar positions in the two complexes, which is quite surprising considering that four of them (Lys249, Cys253, Phe319, and Gln315) interact directly with the nucleobase, which is present in one end-product structure and absent in the other. The phosphodiesters 5′ to the lesion are held in nearly identical positions through a hydrogen bonding interaction with His270 (data not shown in Figure 4), though the nonbridging oxygens are shifted slightly due to vicinal bond rotations. The phosphate (end product, **6**) or phosphodiester (religated product, **8**) immediately 3′ to the lesion is also relatively fixed in position in the two end-product structures, and retains its coordination to a divalent metal ion (Ca^{2+} in our structures) that makes several additional inner- and outer-sphere interactions with the protein and DNA. The major differences between the two end-product structures are in the connectivity and conformation of the lesion sugar moiety. In the abasic end-product complex, the DDR moiety is shifted toward the base-recognition pocket, with the 1′-OH occupying roughly the same space as C8 of the nucleobase. The DDR moiety would thus have to move from the observed position, in the presence of a nucleobase. The conformation of the restored backbone in the aminoG-containing end-product complex is typical of that observed in other hOgg1 structures containing a ring-opened sugar and intact backbone [15] (heavy atom rmsds = 0.62 to ~0.65 Å).

Reaction Chemistry

The DDR moiety is not unexpected as an end product of DNA strand cleavage catalyzed by D268E hOgg1. We envision that the α,β-unsaturated Schiff base **5**, an intermediate that has been observed by borohydride-trapping [15], undergoes hydrolysis to give the corresponding α,β-unsaturated aldehyde liberating Lys249 as a free amine. The α,β-unsaturated aldehyde then undergoes spontaneous ring closure to furnish the DDR end product **6**. The double bond geometry of **5** is not known; if the double bond is configurated *trans* (not *cis* as shown in Figure 1), it would have to isomerize prior to ring closure, because a *trans* double bond cannot exist in a 5-membered ring, owing to ring strain. Such an isomerization could foreseeably take place at the stage of either **5** or the α,β-unsaturated aldehyde due to relatively acidic C2′ hydrogens in these species.

More than one candidate pathway exists for the conversion of **6** to the religated product **8**; the actual pathway cannot be unambiguously defined at this stage. Loading of aminoG onto **6** could result in simple reversal of the steps **6**→**5**→**4**→**3** (but with aminoG in place of oxoG), followed by hydrolysis of the Schiff base to give **8** (or the corresponding C1′-hydrated form). Alternatively, the ring-opened α,β-unsaturated aldehyde **7** might undergo conjugate addition [18, 19] by the 3′-phosphate before Schiff base formation. In this latter pathway, electrophilic activation might be provided by hydrogen bonding between the 1′ carbonyl oxygen and the N-9H of aminoG, a reaction process akin to the nucleobase-assisted catalysis that facilitates the normal repair reaction [11]. It is noteworthy that neither **6** nor **8** contain a covalent linkage between the end product and Lys249, indicating that the hydrolysis of such linkages is thermodynamically favored. It is unclear why the religated product does not simply undergo strand cleavage once again. Either the religated product becomes trapped kinetically, or this product is thermodynamically preferred under the conditions of crystal soaking. Neither of these explanations is completely satisfactory, since the long time scale of crystallography usually disfavors observation of kinetically trapped

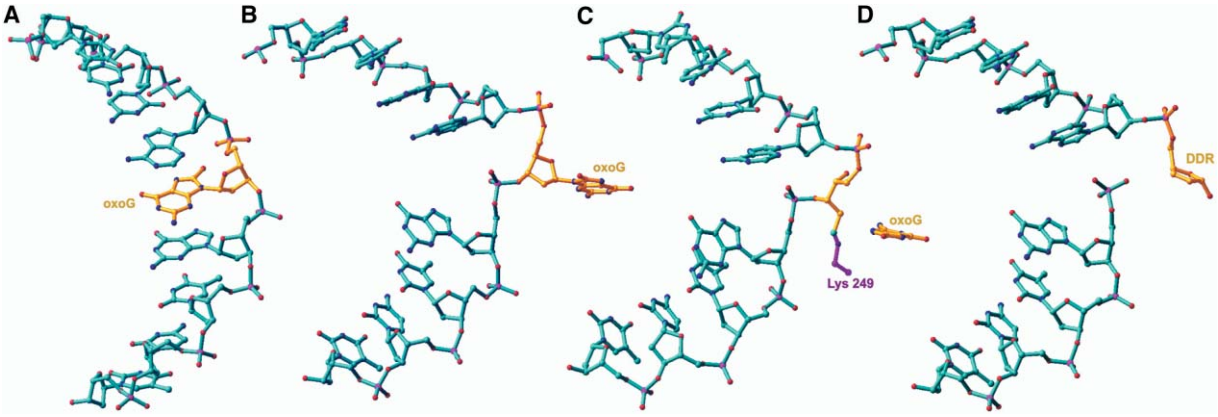

Figure 5. Alterations of DNA Structure during hOgg1-Catalyzed Processing

Only the lesion-containing strand is shown.

(A) An oxoG lesion prior to binding of hOgg1, modeled as B-DNA; oxoG is known not to distort the helical structure of DNA [21, 22].

(B) DNA from the lesion recognition complex of K249Q hOgg1 [10] bound to an intact oxoG-containing duplex.

(C) Energy-minimized model of the Schiff base intermediate **3** [15], based upon from the X-ray structure of the borohydride-trapped complex.

(D) DNA in the end-product complex (this work).

species, and, in solution under single turnover conditions, aminoG accelerates DNA cleavage by D268E hOgg1, quantitatively generating the strand-cleaved DNA product [14]. Whichever is the case, this unusual religation reaction in the crystal would not take place, nor would the product persist, were it not for the unique chemical microenvironment provided by the enzyme active site.

The end-product and religated structures reported here are those formed by a mutant form of hOgg1 having the catalytic Asp268 residue mutated to Glu. Furthermore, the religated product **8** is formed in the presence of a purine analog, aminoG, rather than with the physiologic ligand, oxoG. The question naturally arises as to whether these same end products would be formed with wild-type hOgg1 utilizing an oxoG nucleobase. We cannot provide a definitive answer for this question, but we do note that the D268E mutant of hOgg1 is as active as wild-type for both base excision and strand cleavage [14], and that aminoG in DNA is a substrate for the base-excision activity of wild-type hOgg1 [20]; more importantly, aminoG acts as an effective cofactor to accelerate strand cleavage by wild-type (and D268E) hOgg1 [14, 15]. We do note that in the end-product crystals formed with the wild-type hOgg1, the lesion-recognition pocket is only partially occupied by oxoG, which could explain the observation of multiple species in the sugar portion of the product.

Changes in DNA Structure during hOgg1-Catalyzed Processing of a Lesion

The availability of X-ray structures [10, 15] and molecular models [15] representing multiple states of the hOgg1 lesion-processing reaction allows us to begin developing a detailed depiction of the structural changes in the substrate DNA accompanying this complex biochemical process. hOgg1 initially binds duplex DNA containing an intrahelical oxoG lesion (Figure 5A); the lesion is known not to cause distortion of the DNA helix [21, 22]. In a process that remains poorly understood, the protein then causes extrusion of the oxoG nucleoside from a DNA helix that now contains a sharp localized bend (Figure 5B). This overall geometry of the DNA appears to be preserved through the chemical steps of the repair reaction, during which the covalent structure of the lesion is altered within the confines of the active site (Figures 5C and 5D). It is likely that a significant amount of strain energy is released in the sharply bent DNA helix as the oxoG base is expelled and backbone is cleaved, thereby decreasing the overall free energy state of the final product DNA/hOgg1 complex. Perhaps this decrease in strain energy is what enables hOgg1 to remain tightly associated with its end product.

Significance

DNA glycosylase/lyases are key players in the cellular defense against the genotoxic effects of DNA damage. These proteins are remarkably versatile, catalyzing a reaction cascade that begins with excision of a damaged base from the genome and ultimately leads cleavage of the DNA backbone. Considerable interest surrounds the mechanism by which DNA glycosylase/lyases perform such a marvel of catalysis. Previous studies focusing on human 8-oxoguanine DNA glycosylase (hOgg1) have led to a detailed proposal for the reaction mechanism [8, 10], the initial stages of which have received strong support from high-resolution crystallographic structures [10, 11, 14]. Structural information on the later stages of the cascade has, however, been lacking to date. Here, we report an X-ray structure of a late reaction intermediate, namely the final end product of DNA lesion processing by the enzyme. This structure lends key support to the proposed mechanism of the DNA strand cleavage pathway, and leads to a model wherein release of conformational strain energy in the DNA helix en-

Table 1. Data Collection and Model Statistics

Data Collection (Å)	End Product	Religated Structure
Resolution	50–2.05	50–1.90
Unique reflections	32,927	42,539
Redundancy	5.2	5.2
Completeness (%)[a]	97.9 (88.4)	99.4 (99.1)
R_{merge}[a,b]	0.07 (0.612)	0.067 (0.470)
$<I/\sigma>$	23.1 (2.1)	23.7 (2.3)
Refinement and Model Statistics		
Resolution (Å)	2.30	1.90
R_{cryst}[a,c]	23.0 (26.9)	23.4 (28.6)
R_{free}[a,c]	27.4 (32.7)	26.8 (31.5)
Mean B value, all atoms (Å^2)	49.4	41.6
Rmsd from ideality:		
Bond lengths (Å)	0.006	0.006
Bond angles (°)	1.2	1.4
Dihedral angles (°)	20.7	21.5
Ramachandran plot		
Most favored	89.4%	92.3%
Additionally allowed	9.9%	7.4%
Generously allowed[d]	0.7%	0.4%
Protein and DNA atoms	3047	3052
Waters	93	173

[a] Values in parentheses refer to the highest resolution bin.
[b] $R_{merge} = \Sigma_{hkl} |I(hkl) - <I(hkl)>|/\Sigma_{hkl} |<I(hkl)>|$.
[c] $R_{cryst} = \Sigma_{hkl} |F_o(hkl) - F_c(hkl)>|/\Sigma_{hkl} |F_o(hkl)|$. R_{free} was calculated based on 10% of the total data omitted during the structure refinement [26].
[d] Asp174 in both structures and Leu 170 in end-product structure fell in this region of phi-psi space in all structures. It was visually inspected using the final σA weighted $2F_o - F_c$ map and observed to be correctly positioned.

ables hOgg1 to remain bound tightly to its final reaction product. Serendipitously, we observed religation of the DNA backbone when an oxoguanine analog, 8-aminoG, was soaked into the enzyme active site. This observation provides further evidence for the role of the excised base (8-oxoG) as a cocatalyst in the hOgg1-catalyzed lyase reaction [11].

Experimental Procedures

Crystallization, Data Collection, and Structure Determination

Crystallization of the end-product complex followed closely that described for the lesion-recognition complex [10] except the mixture of protein and DNA was allowed to incubate for 2 hr at 4°C before hanging drops were set up. Crystals grew in 1–3 days at 4°C. Prior to freezing in liquid nitrogen, end-product crystals were briefly soaked in crystallization buffer supplemented with 25% glycerol. To generate the religated complex, crystals of the end-product complex were soaked overnight in crystallization buffer supplemented with 25% glycerol and 2 mM aminoG. X-Ray diffraction data (λ = 0.930) were collected at the F1 beam line of CHESS (Cornell High-Energy Synchrotron Source) on an ADSC CCD detector. Diffraction data were processed using the DENZO/SCALEPACK software package [23]. Structures were refined starting from the K249Q hOgg1/DNA complex structure (PDB ID: 1EBM) using CNS 1.0 [24]. Model statistics and geometries (calculated using PROCHECK) [25] are presented in Table 1.

Acknowledgments

We are grateful to J. Christopher Fromme for assistance with data collection and processing, and for sharing unpublished data and helpful discussions. We acknowledge Derek P.G. Norman for sharing unpublished data and helpful discussions. We thank Chris Heaton and the entire MacCHESS staff for assistance with data collection. This work was supported by a grant from the NIH (CA100742).

Received: August 25, 2003
Revised: August 30, 2004
Accepted: September 27, 2004
Published: December 17, 2004

References

1. Friedberg, E.C., Walker, G.C., and Siede, W. (1995). DNA Repair and Mutagenesis (Washington DC: American Society for Microbiology).
2. Hollis, T., Lau, A., and Ellenberger, T. (2001). Crystallizing thoughts about DNA base excision repair. Prog. Nucleic Acid Res. Mol. Biol. *68*, 305–314.
3. David, S.S., and Williams, S.D. (1998). Chemistry of glycosylases and endonucleases involved in base-excision repair. Chem. Rev. *98*, 1221–1261.
4. Scharer, O.D., and Jiricny, J. (2001). Recent progress in the biology, chemistry and structural biology of DNA glycosylases. Bioessays *23*, 270–281.
5. Dodson, M.L., Michaels, M.L., and Lloyd, R.S. (1994). Unified catalytic mechanism for DNA glycosylases. J. Biol. Chem. *269*, 32709–32712.
6. Schrock, R.D., III, and Lloyd, R.S. (1991). Reductive methylation of the amino terminus of endonuclease V eradicates catalytic activities. Evidence for an essential role of the amino terminus in the chemical mechanisms of catalysis. J. Biol. Chem. *266*, 17631–17639.
7. Tchou, J., and Grollman, A.P. (1995). The catalytic mechanism of Fpg protein. Evidence for a Schiff base intermediate and amino terminus localization of the catalytic site. J. Biol. Chem. *270*, 11671–11677.
8. Nash, H.M., Lu, R., Lane, W.S., and Verdine, G.L. (1997). The critical active-site amine of the human 8-oxoguanine DNA glycosylase, hOgg1: direct identification, ablation and chemical reconstitution. Chem. Biol. *4*, 693–702.
9. Sun, B., Latham, K.A., Dodson, M.L., and Lloyd, R.S. (1995). Studies on the catalytic mechanism of five DNA glycosylases. Probing for enzyme-DNA imino intermediates. J. Biol. Chem. *270*, 19501–19508.

10. Bruner, S.D., Norman, D.P.G., and Verdine, G.L. (2000). Structural basis for recognition and repair of the endogenous mutagen 8-oxoguanine in DNA. Nature *403*, 859–866.
11. Fromme, J.C., and Verdine, G.L. (2002). Structural insights into lesion recognition and repair by the bacterial 8-oxoguanine DNA glycosylase MutM. Nat. Struct. Biol. *9*, 544–552.
12. Zharkov, D.O., Golan, G., Gilboa, R., Fernandes, A.S., Gerchman, S.E., Kycia, J.H., Rieger, R.A., Grollman, A.P., and Shoham, G. (2002). Structural analysis of an Escherichia coli endonuclease VIII covalent reaction intermediate. EMBO J. *21*, 789–800.
13. Norman, D.P.G., Bruner, S.D., and Verdine, G.L. (2001). Coupling of substrate recognition and catalysis by a human base-excision DNA repair protein. J. Am. Chem. Soc. *123*, 359–360.
14. Norman, D.P.G., Chung, S.J., and Verdine, G.L. (2003). Structural and biochemical exploration of a critical amino acid in human 8-oxoguanine glycosylase. Biochemistry *42*, 1564–1572.
15. Fromme, J.C., Bruner, S.D., Yang, W., Karplus, M., and Verdine, G.L. (2003). Product-assisted catalysis in base-excision DNA repair. Nat. Struct. Biol. *10*, 204–211.
16. Chen, L., Haushalter, K.A., Lieber, C.M., and Verdine, G.L. (2002). Direct visualization of a DNA glycosylase searching for damage. Chem. Biol. *9*, 345–350.
17. Vidal, A.E., Hickson, I.D., Boiteux, S., and Radicella, J.P. (2001). Mechanism of stimulation of the DNA glycosylase activity of hOGG1 by the major human AP endonuclease: bypass of the AP lyase activity step. Nucleic Acids Res. *29*, 1285–1292.
18. Moe, O.A., and Warner, D.T. (1949). 1,4-Addition reactions. III. The addition of cyclic imides to α,β,-unsaturated aldehydes. A synthesis of β-alaninine hydrochloride. J. Am. Chem. Soc. *71*, 1251–1253.
19. Hofstraat, R.G., Lange, J., Scheeren, H.W., and Nivard, R.J.F. (1988). Chemistry of ketene acetals. Part 9. A simple one-pot synthesis of 4-hydroxy-δ-lactones and 5,6-dihydro-2-pyrones from 1,1-dimethoxypropene and β-oxy aldehydes. J. Chem. Soc., Perkin Trans. 1 *1*, 2315–2322.
20. Zharkov, D.O., Rosenquist, T.A., Gerchman, S.E., and Grollman, A.P. (2000). Substrate specificity and reaction mechanism of murine 8-oxoguanine-DNA glycosylase. J. Biol. Chem. *275*, 28607–28617.
21. Oda, Y., Uesugi, S., Ikehara, M., Nishimura, S., Kawase, Y., Ishikawa, H., Inoue, H., and Ohtsuka, E. (1991). NMR studies of a DNA containing 8-hydroxydeoxyguanosine. Nucleic Acids Res. *19*, 1407–1412.
22. Lipscomb, L.A., Peek, M.E., Morningstar, M.L., Verghis, S.M., Miller, E.M., Rich, A., Essigmann, J.M., and Williams, L.D. (1995). X-ray structure of a DNA decamer containing 7,8-dihydro-8-oxoguanine. Proc. Natl. Acad. Sci. USA *92*, 719–723.
23. Otwinowski, Z., and Minor, W. (1997). Processing of X-ray diffraction data collected in oscillation mode. Methods Enzymol. *276*, 307–326.
24. Brunger, A.T., Adams, P.D., Clore, G.M., DeLano, W.L., Gros, P., Grosse-Kunstleve, R.W., Jiang, J.-S., Kuszewski, J., Nilges, N., Pannu, N.S., et al. (1998). Crystallography and NMR system (CNS): a new software system for macromolecular structure determination. Acta Crystallogr. D Biol. Crystallogr. *54*, 905–921.
25. Laskowski, R.A., MacArthur, M.W., Moss, D.S., and Thornton, J.M. (1993). PROCHECK: a program to check the stereochemical quality of protein structures. J. Appl. Crystallogr. *26*, 283–291.
26. Brunger, A.T. (1993). Assessment of phase accuracy by cross validation: the free R value. Methods and applications. Acta Crystallogr. D Biol. Crystallogr. *49*, 24–36.
27. Read, R.J. (1986). Improved Fourier coefficients for maps using phases from partial structures with errors. Acta Crystallogr. A *42*, 140–149.

Accession Numbers

Atomic coordinates have been deposited in the Protein Data Bank (accession codes 1M3H [end product] and 1M3Q [religated structure]).